Figure S1

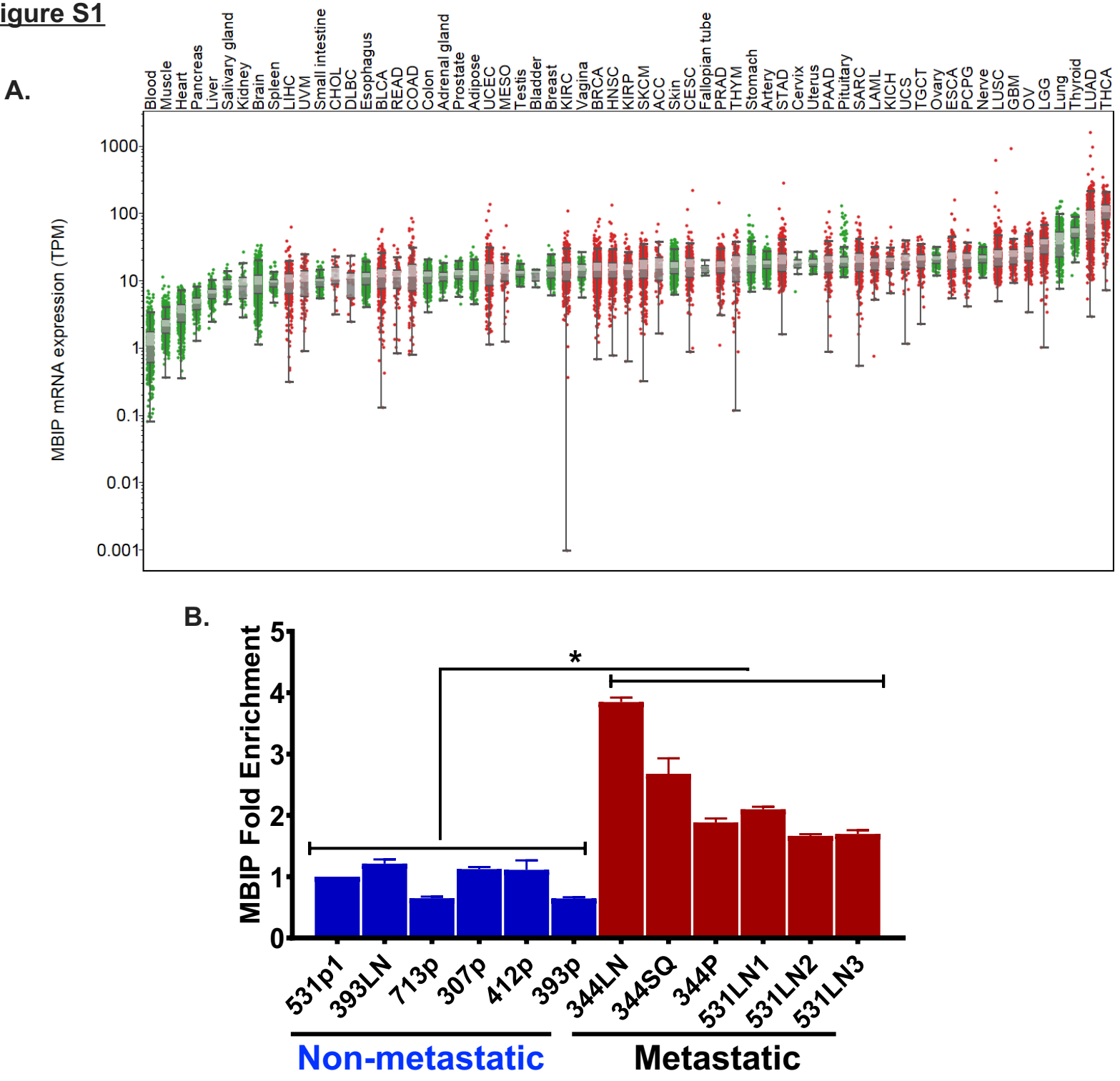

Figure S1. **(A)** MBIP mRNA expression profile in different organs and tumors (including LUAD) in TCGA datasets. **(B)** MBIP expression levels in KP mouse cell panel distinguished based on metastatic ability. MBIP showed increased expression in metastatic cells undergoing EMT compared to non-metastatic/epithelial cells.

Figure S2

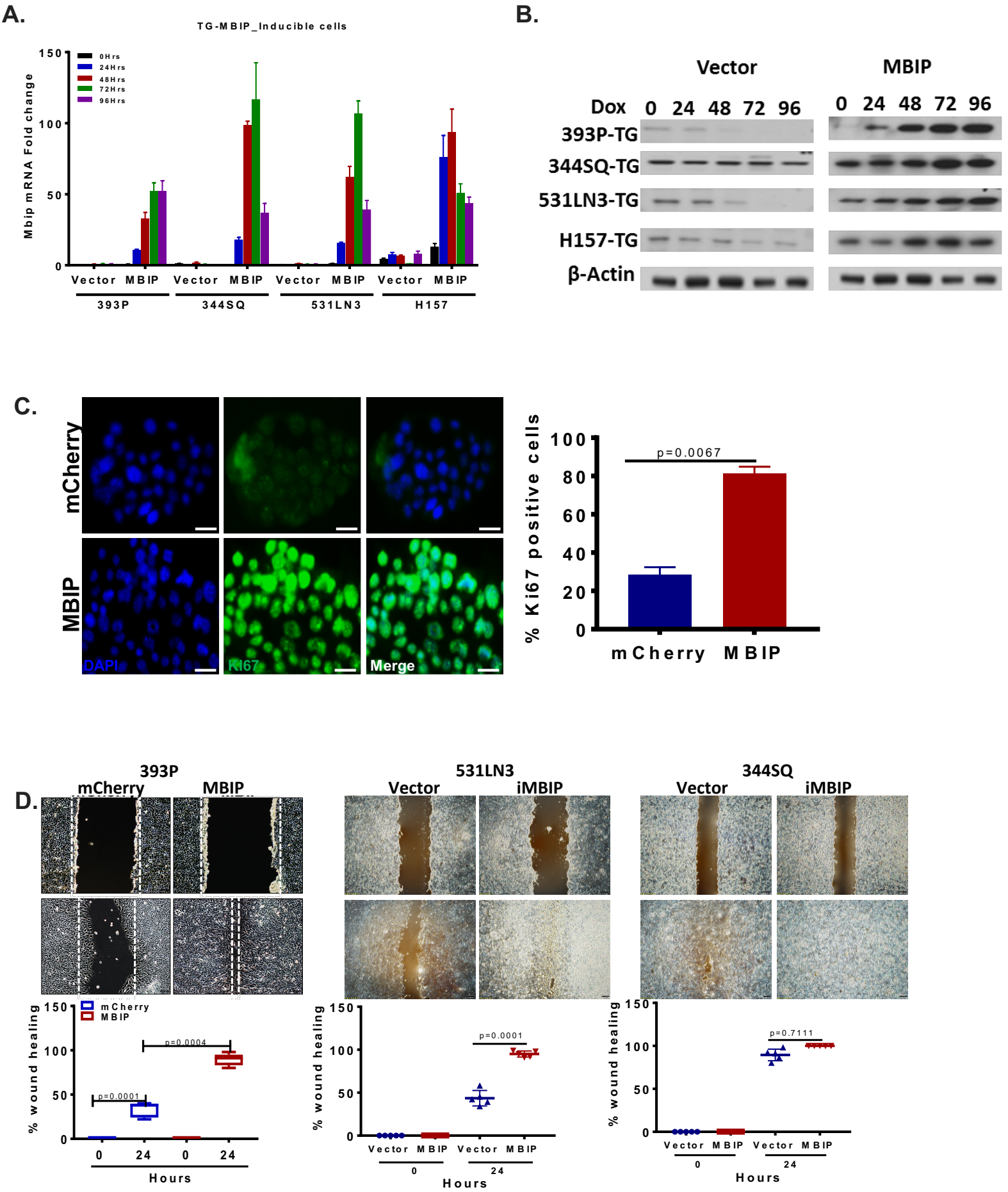
A.
TG-MBIP_Inducible cells
Mbip mRNA Fold change
0Hrs
24Hrs
48Hrs
72Hrs
96Hrs
Vector MBIP Vector MBIP Vector MBIP Vector MBIP
393P
344SQ
531LN3
H157
B.
Vector
MBIP
Dox 0 24 48 72 96
393P-TG
344SQ-TG
531LN3-TG
H157-TG
β-Actin
C.
mCherry
MBIP
DAPI
KI67
Merge
% Ki67 positive cells
p=0.0067
mCherry MBIP
D.
393P
mCherry
MBIP
531LN3
Vector
iMBIP
344SQ
Vector
iMBIP
% wound healing
mCherry
MBIP
p=0.0004
p=0.0001
Hours
p=0.0001
p=0.7111

Figure S2

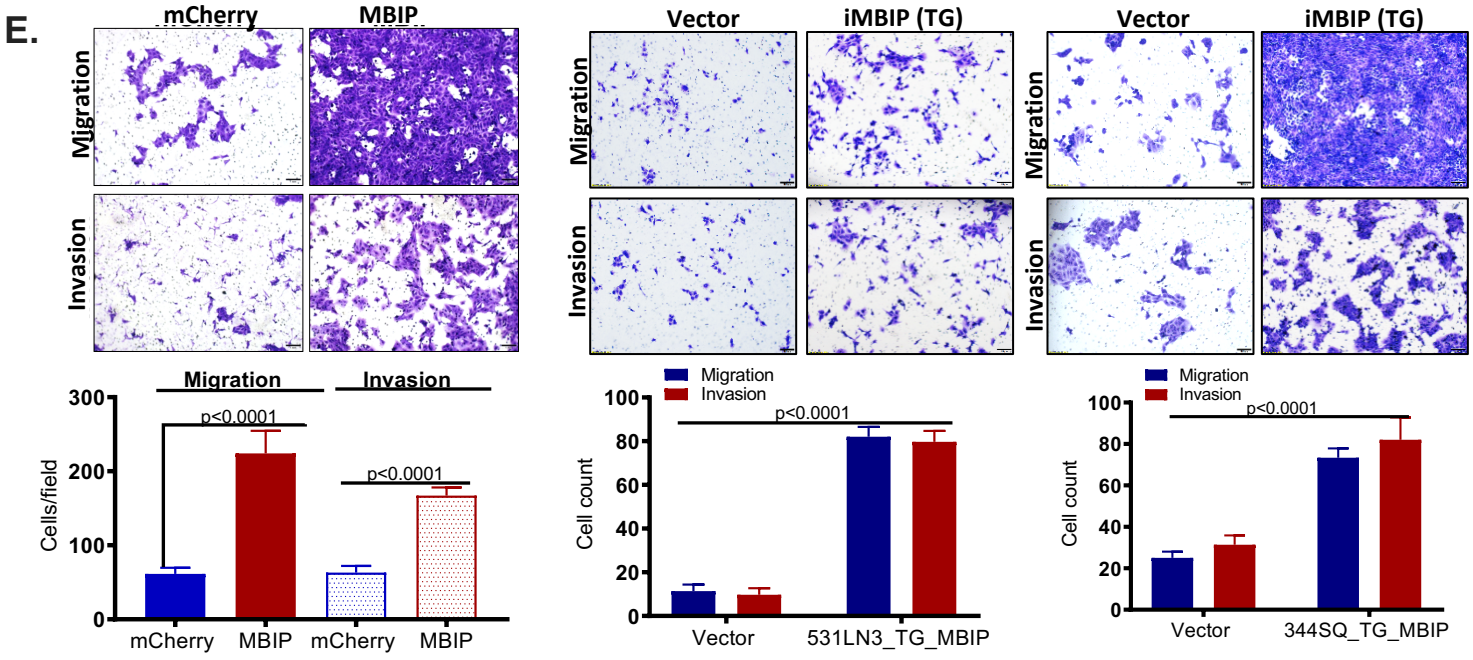

F. **Additional images of 2D for migration and invasion fields in MBIP overexpressing cells.**

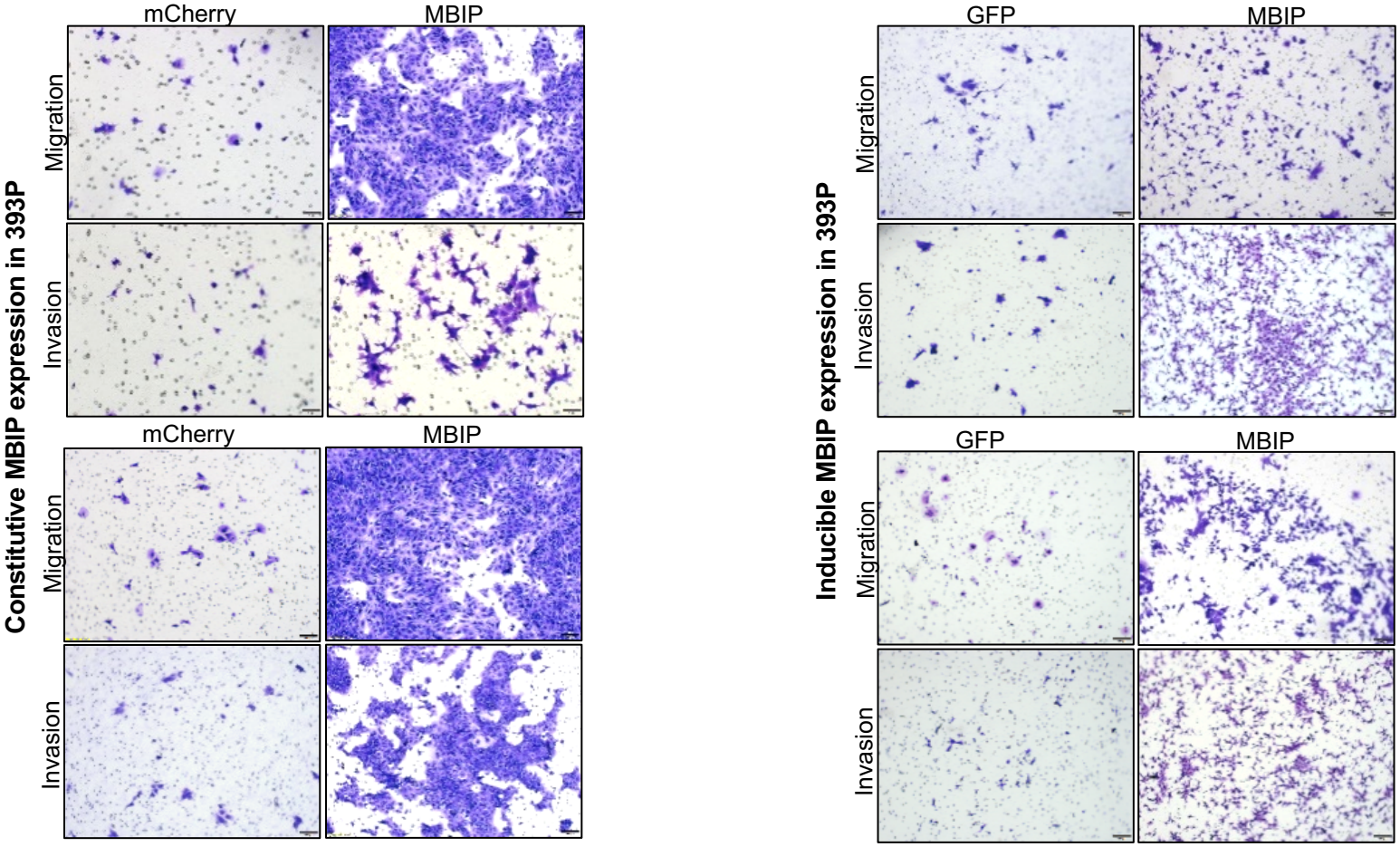

Figure S2

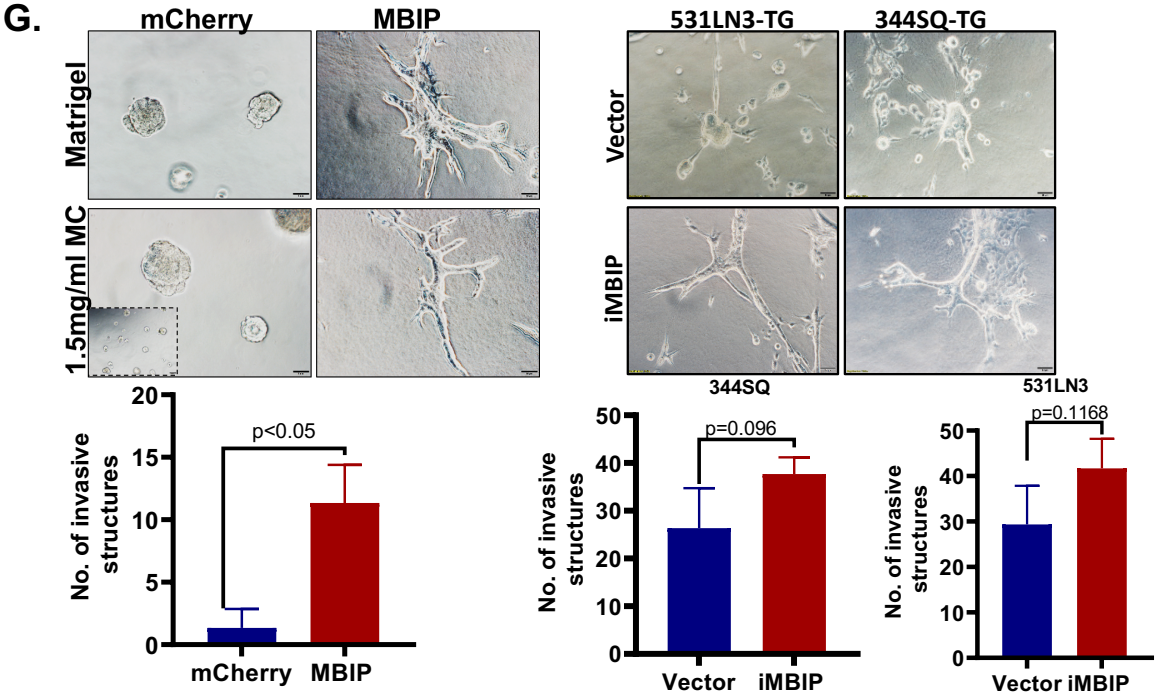

H. Additional images of 3D invasion assays for MBIP overexpressing cells grown in matrix (1.5mg Matrigel:Collagen)

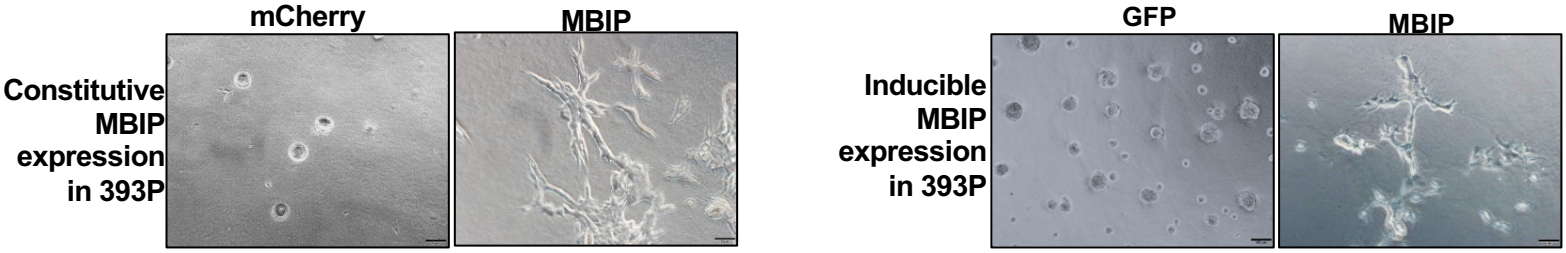

I.

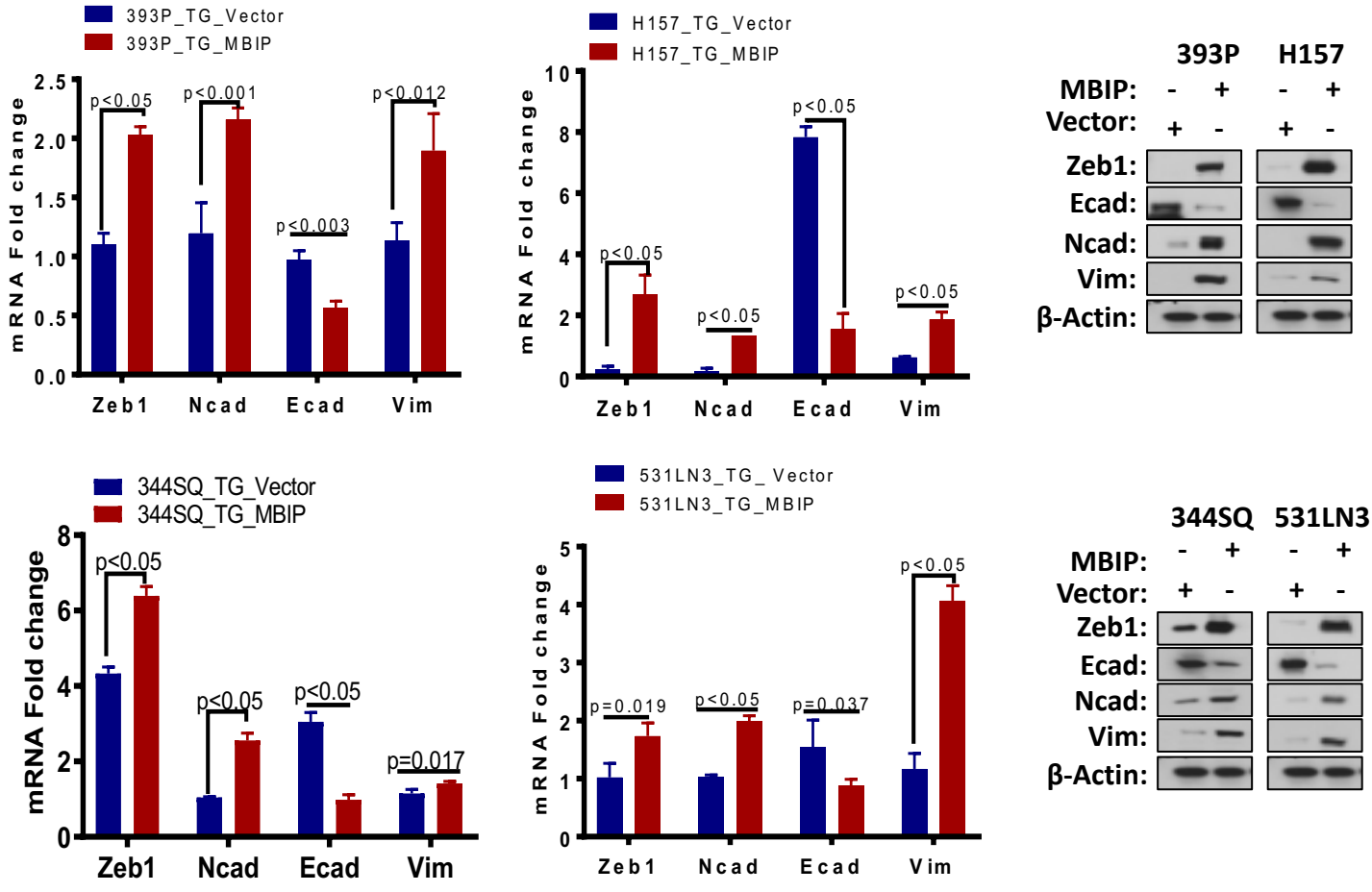

Figure S2

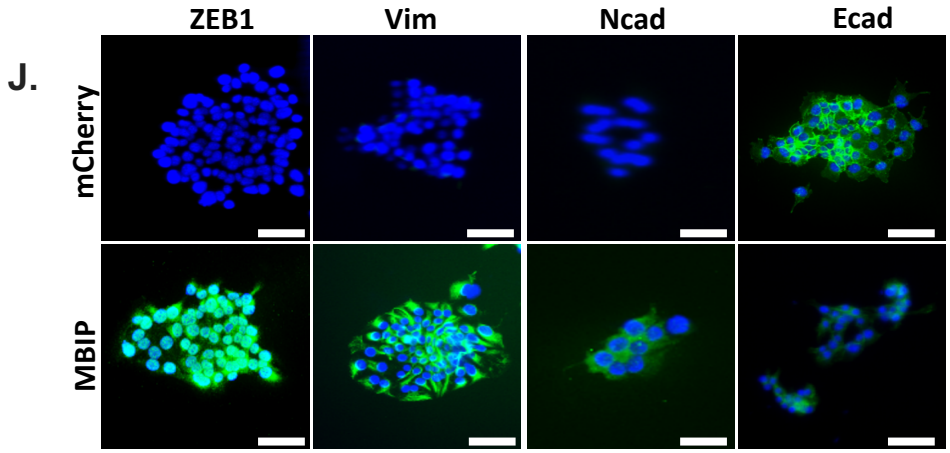
J.
ZEB1
Vim
Ncad
Ecad
mCherry
MBIP

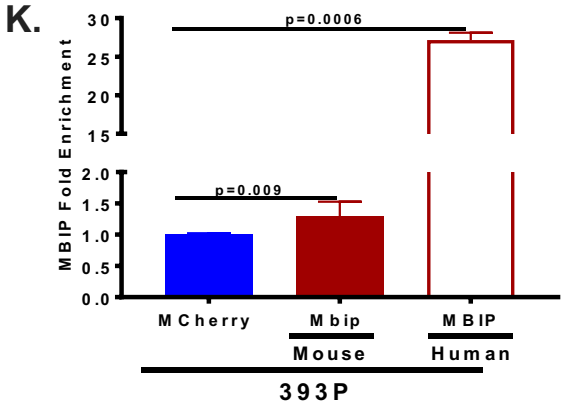
K.
MBIP Fold Enrichment
p=0.0006
p=0.009
MCherry
Mbip
MBIP
Mouse
Human
393P

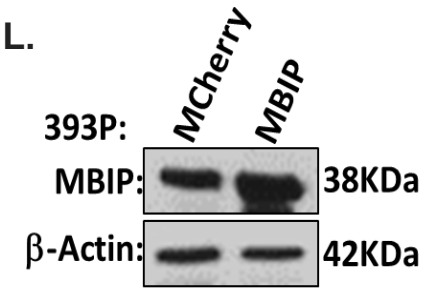
L.
393P:
MCherry
MBIP
MBIP:
38KDa
β-Actin:
42KDa

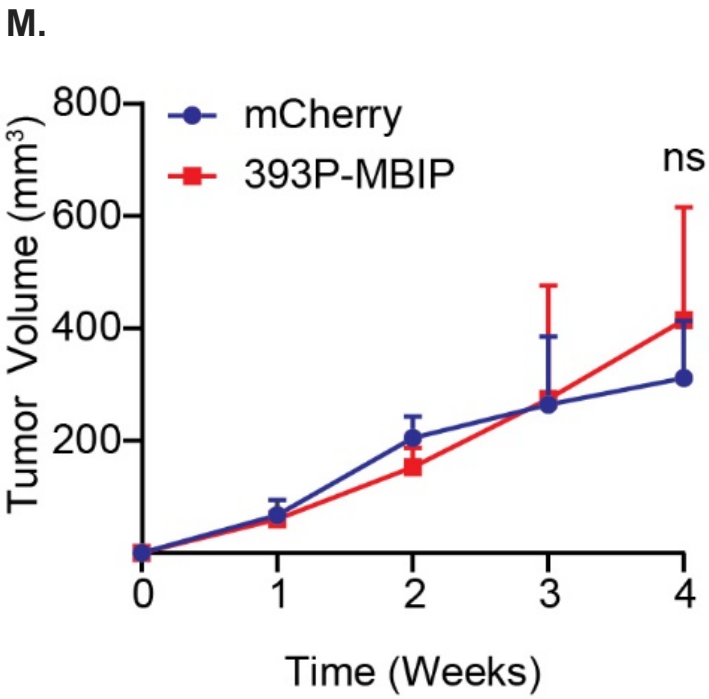
M.
Tumor Volume (mm3)
mCherry
393P-MBIP
ns
Time (Weeks)

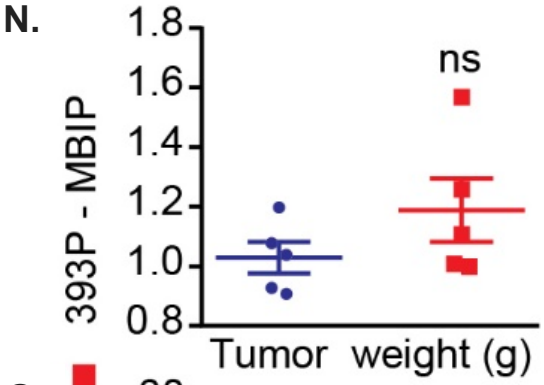
N.
393P - MBIP
ns
Tumor weight (g)

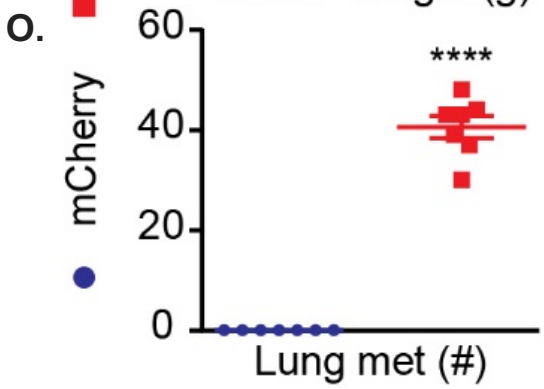
O.
mCherry
****
Lung met (#)

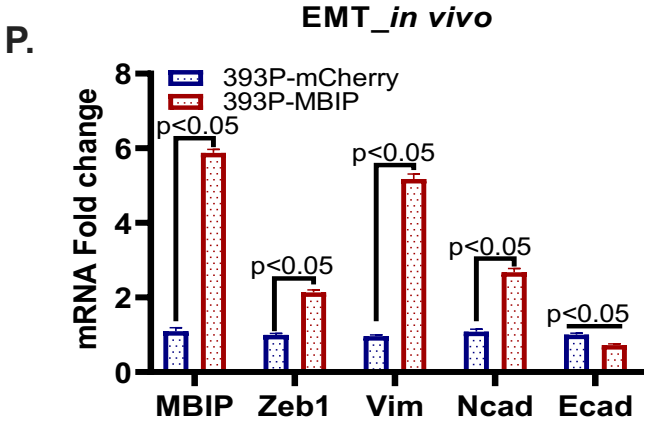
P.
EMT_in vivo
393P-mCherry
393P-MBIP
mRNA Fold change
p<0.05
MBIP
Zeb1
Vim
Ncad
Ecad

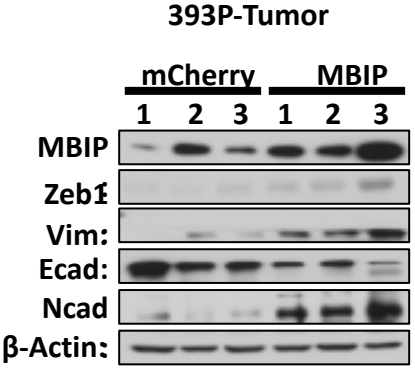
393P-Tumor
mCherry
MBIP
1 2 3 1 2 3
MBIP
Zeb1
Vim:
Ecad:
Ncad
β-Actin:

Figure S2. **(A)** Transcript levels of MBIP in 393P, 344SQ, 531LN3, H157 cells with inducible-overexpression of MBIP, determined by qRT–PCR and compared to non-doxycycline treated cells as controls. Error bars indicate ±SEM, *n*= 3 experiments **(B)** Immunoblot analysis of MBIP in cells as described in (C). β-Actin loading control is shown (bottom panel). **(C)** Representative images of immunofluorescent (IF) staining for Ki67, was used to determine proliferation in MBIP-overexpressing 393P cells, compared with mCherry control cells. The quantification of Ki67 positive cells is shown. Nucleus was stained with DAPI. Increased Ki67 staining was seen in MBIP-overexpressing cells. **(D)** Doxycycline-inducible MBIP-overexpressing 531LN3 and 344SQ cells which were induced for 24 hours, and constitutive MBIP-overexpressing 393P cells, were used for quantification of their invasive and migratory potentials, using Wound healing assays. **(E)** Doxycycline-inducible MBIP-overexpressing 531LN3 and 344SQ cells which were induced for 24 hours, and constitutive MBIP-overexpressing 393P cells, were used for quantification of their invasive and migratory potentials, using Trans-well assays for migration and invasion. Assays demonstrated increased cellular motility, migration, and invasion upon MBIP overexpression. (magnification, ×40). *P<0.0 5. **(F)** Additional representative images for migration and invasion assays by using the constitutive and inducible MBIP-overexpressing 393P cells. **(G)** Representative photographs of 3D matrix with invasive spheroids formed by constitutive MBIP-overexpressing 393P cells (left) and by doxycycline-inducible MBIP-overexpressing 344SQ and 531LN3 cells which were induced for 24 hours (right). Data shows increased formation of invasive spheroids upon MBIP overexpression. Scale bar = 20 μm. **(H)** Additional representative images for 3D collagen/matrigel invasion assay by using the constitutive and inducible MBIP-overexpressing 393P cells. **(I)** RT-qPCR and western blot analysis show MBIP-mediated regulation of EMT in mouse (393P, 344SQ, 531LN3) and human (H157) MBIP-inducible cells. Zeb1, N-cadherin, and Vimentin were used as markers of the mesenchymal state, whereas E-cadherin was used as a marker of the epithelial state. β-Actin was used as a loading control. **(J)** IF staining for EMT markers Zeb1, N-cadherin, Vimentin, and E-cadherin also show MBIP as a regulator of EMT in 393P cells with constitutive MBIP overexpression. **(K)** qRT-PCR analysis for MBIP endogenous mouse and exogenous human levels, in constitutive MBIP-overexpressing 393P cells, relative to mCherry controls **(L)** Immunoblot analysis of MBIP levels. β-Actin loading control is shown in the bottom panel.

Figure S2. (M) Tumor growth in mice injected with 5×10^5 of 393P-MBIP or 1×10^6 of 393P-mCherry control cells. Tumor size was measured every 7 days for 4 weeks. **(N)** Tumor weights measured after subcutaneous tumors were dissected from the tumor-bearing mice that were sacrificed at 4 weeks **(O)** Metastasis was quantified at the time of sacrifice by counting macroscopic lung metastatic nodules. MBIP-overexpressing tumors showed no change in tumor volume but exhibited a significantly higher metastatic potential. Data mean ± SEM. **(P)** RT-qPCR and western blot analysis on tumors collected from mice implanted with control or MBIP 393P cells demonstrate MBIP upregulating EMT *in vivo*. Same EMT markers as described before were used. *P<0.05 compared with the scramble control group, which demonstrate increased motility compared to MBIP knockdown cells.

Figure S3

A.

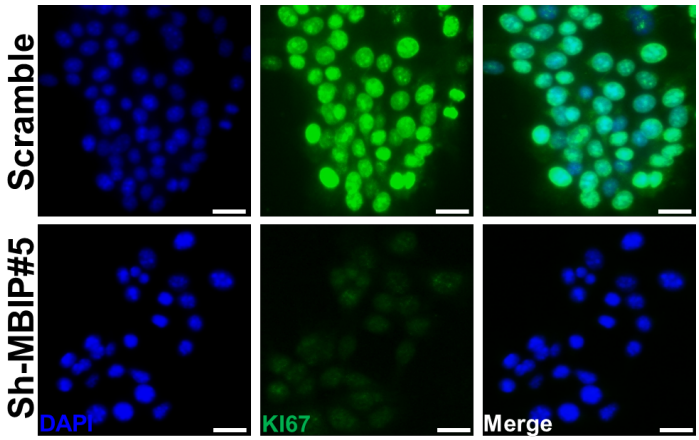

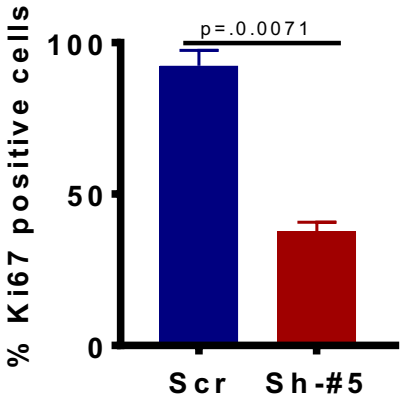

B.

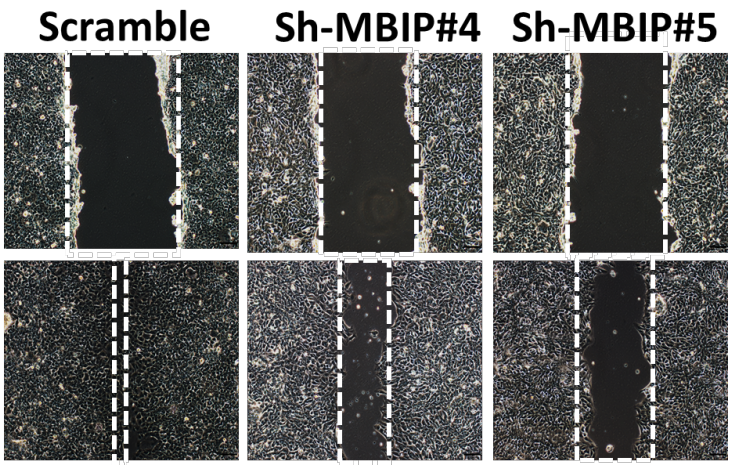

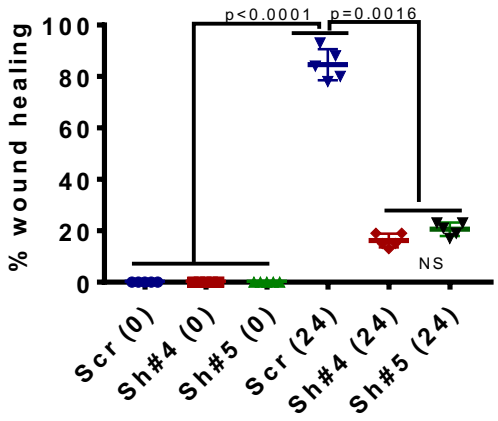

C. **Additional images of 2D for migration and invasion fields in MBIP knockdown cells.**

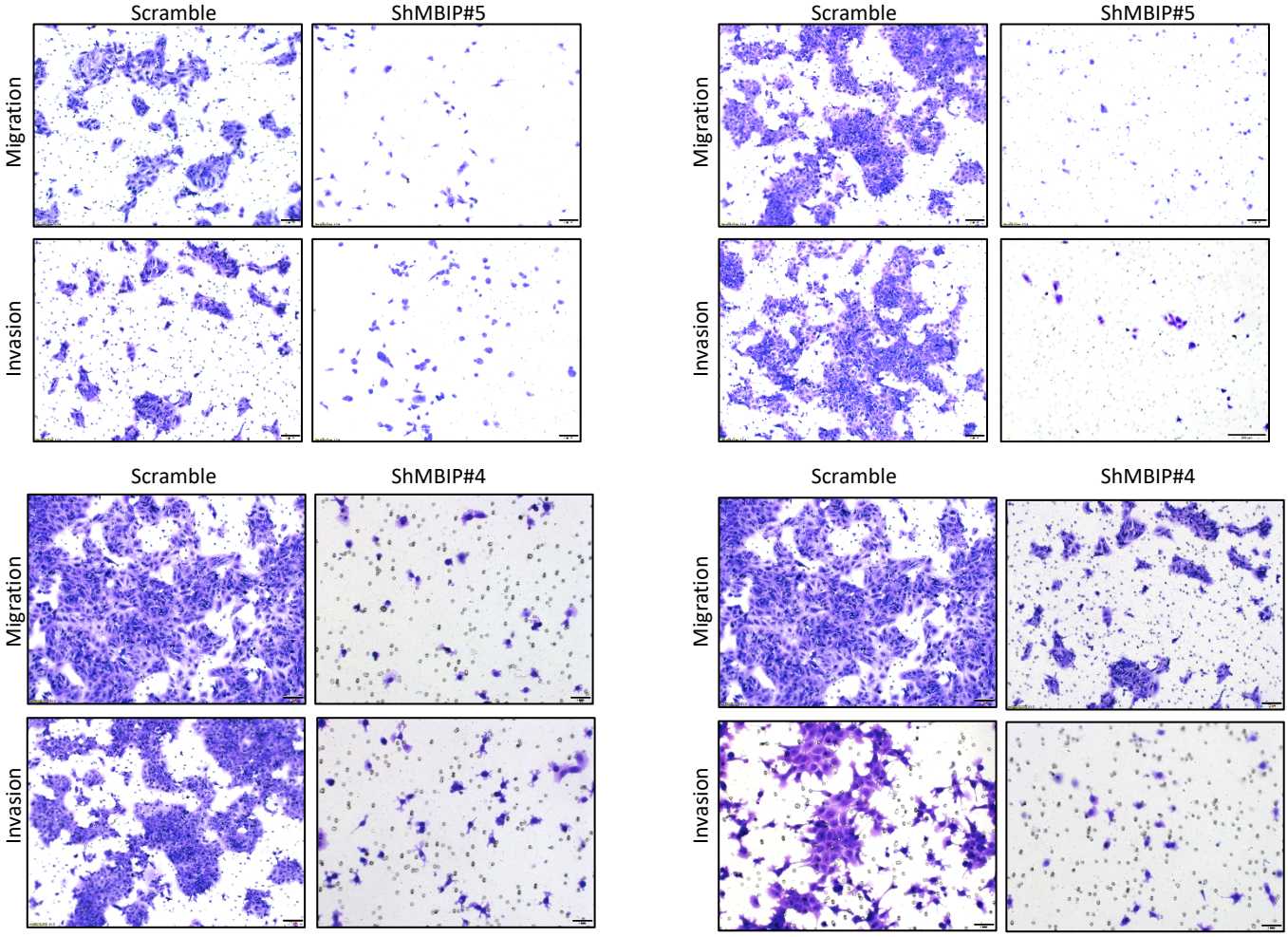

Figure S3

D. Additional images of 3D invasion assays for MBIP knockdown cells.

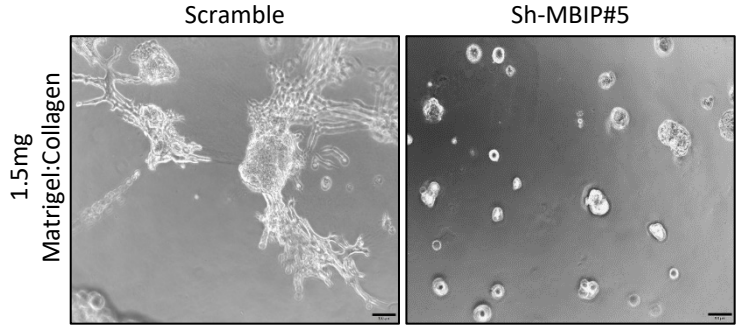

Figure S3. (A) Representative images of immunofluorescent (IF) staining for Ki67, was used to determine proliferation in MBIP-knockdown 344SQ cells as described in Figure S2. Ki67 staining was decreased upon MBIP knockdown. Data is represented as mean ± SEM. *P<0.05, and ***P<0.001. Scale bar = 50 μm. **(B)** Scratch wound healing assays using scramble control and MBIP knockdown cells (magnification, ×40). *P<0.05 compared with the scramble control group, which demonstrate increased motility compared to MBIP knockdown cells. **(C)** Additional representative images for migration and invasion assays using the MBIP-knockdown 344SQ cells. Data is represented as mean ± SEM. *P<0.05, and ***P<0.001. **(D)** Additional representative images for 3D collagen/matrigel invasion assay using the MBIP-knockdown 344SQ cells. Data is represented as mean ± SEM. *P<0.05, and ***P<0.001.

Figure S4

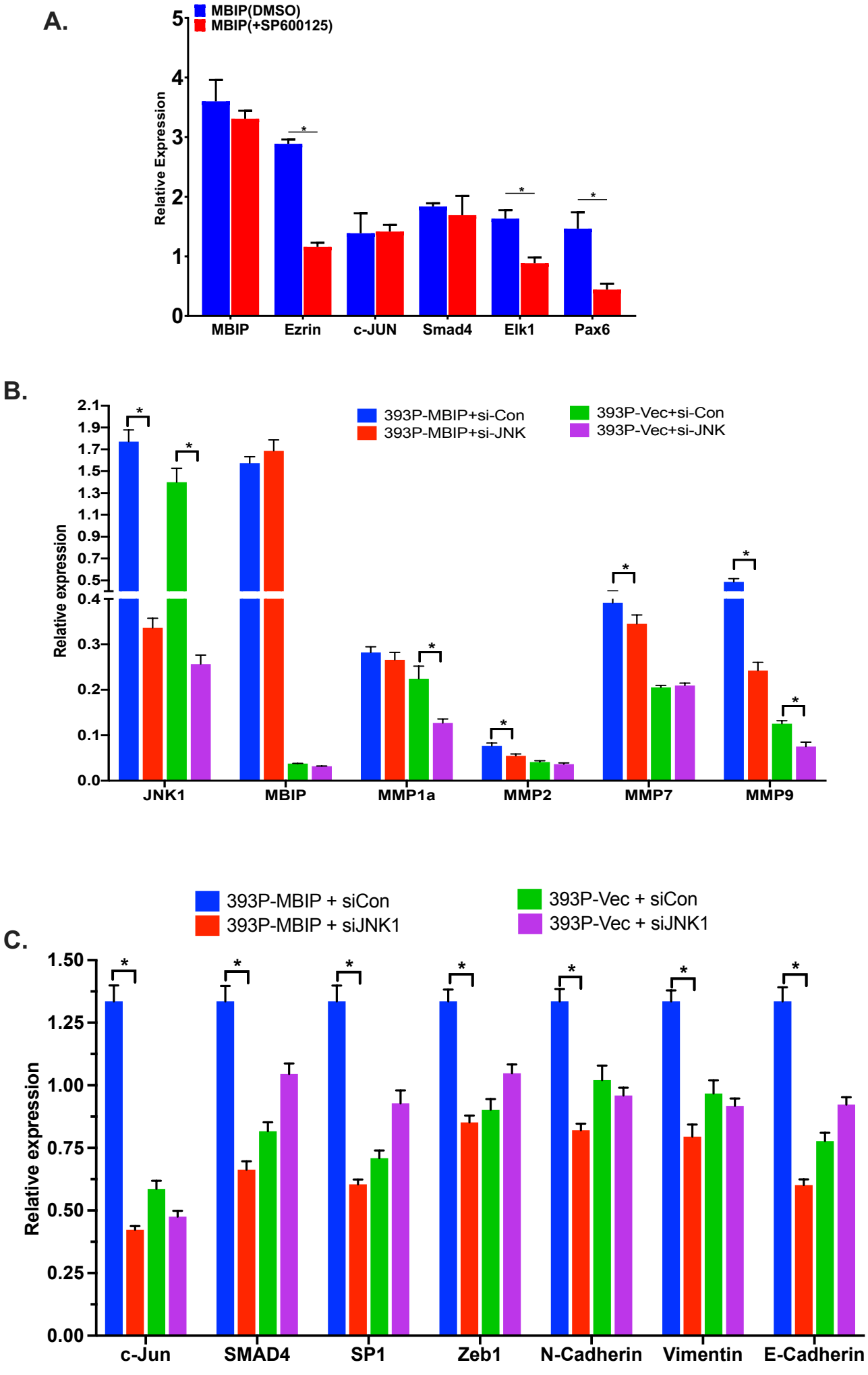
A.
MBIP(DMSO)
MBIP(+SP600125)
Relative Expression
MBIP
Ezrin
c-JUN
Smad4
Elk1
Pax6
B.
393P-MBIP+si-Con
393P-MBIP+si-JNK
393P-Vec+si-Con
393P-Vec+si-JNK
Relative expression
JNK1
MBIP
MMP1a
MMP2
MMP7
MMP9
C.
393P-MBIP + siCon
393P-MBIP + siJNK1
393P-Vec + siCon
393P-Vec + siJNK1
Relative expression
c-Jun
SMAD4
SP1
Zeb1
N-Cadherin
Vimentin
E-Cadherin

Figure S4

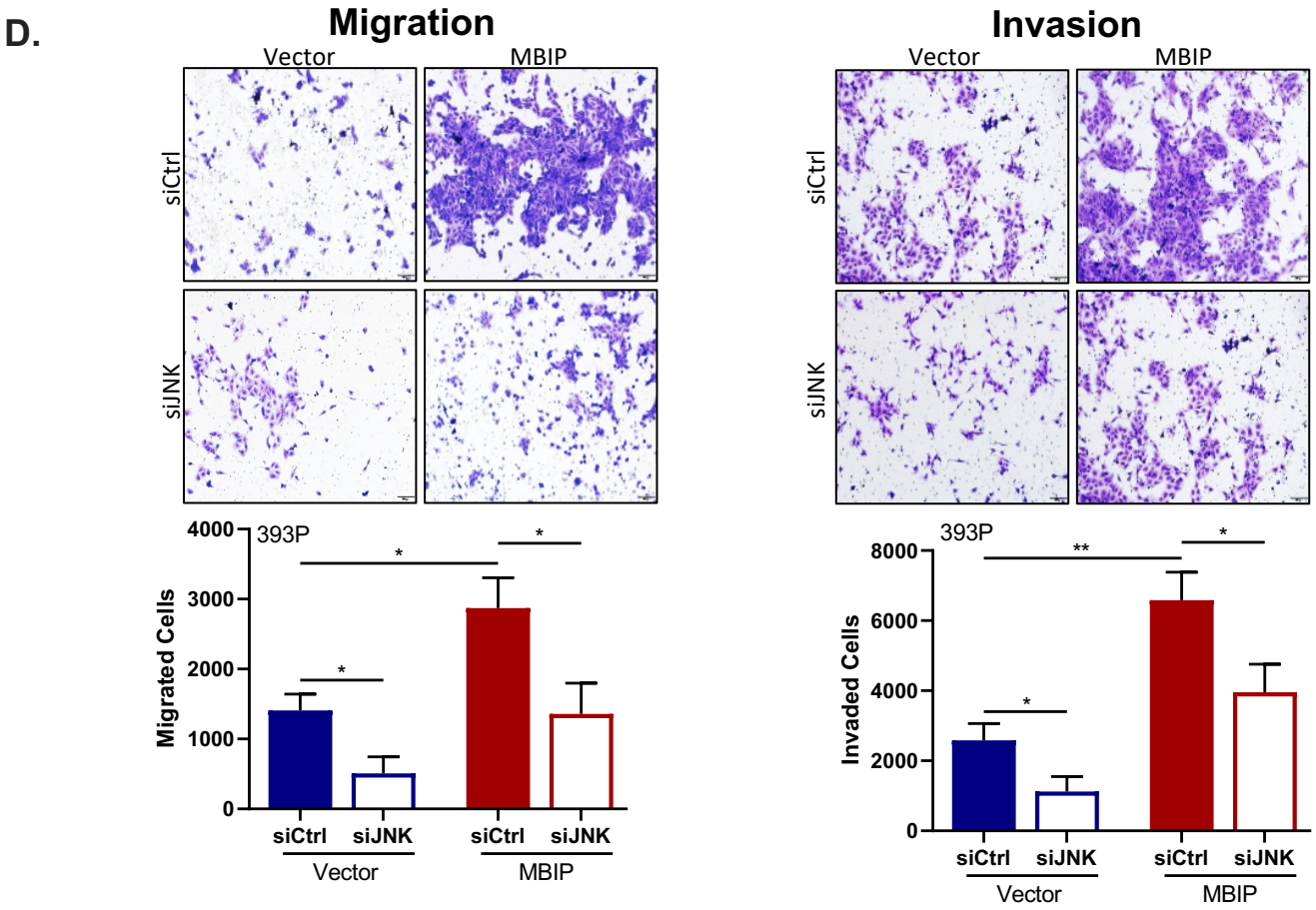
D.
Migration
Vector
MBIP
siCtrl
siJNK
393P
Migrated Cells
4000
3000
2000
1000
0
siCtrl
siJNK
siCtrl
siJNK
Vector
MBIP
Invasion
Vector
MBIP
siCtrl
siJNK
393P
Invaded Cells
8000
6000
4000
2000
0
siCtrl
siJNK
siCtrl
siJNK
Vector
MBIP

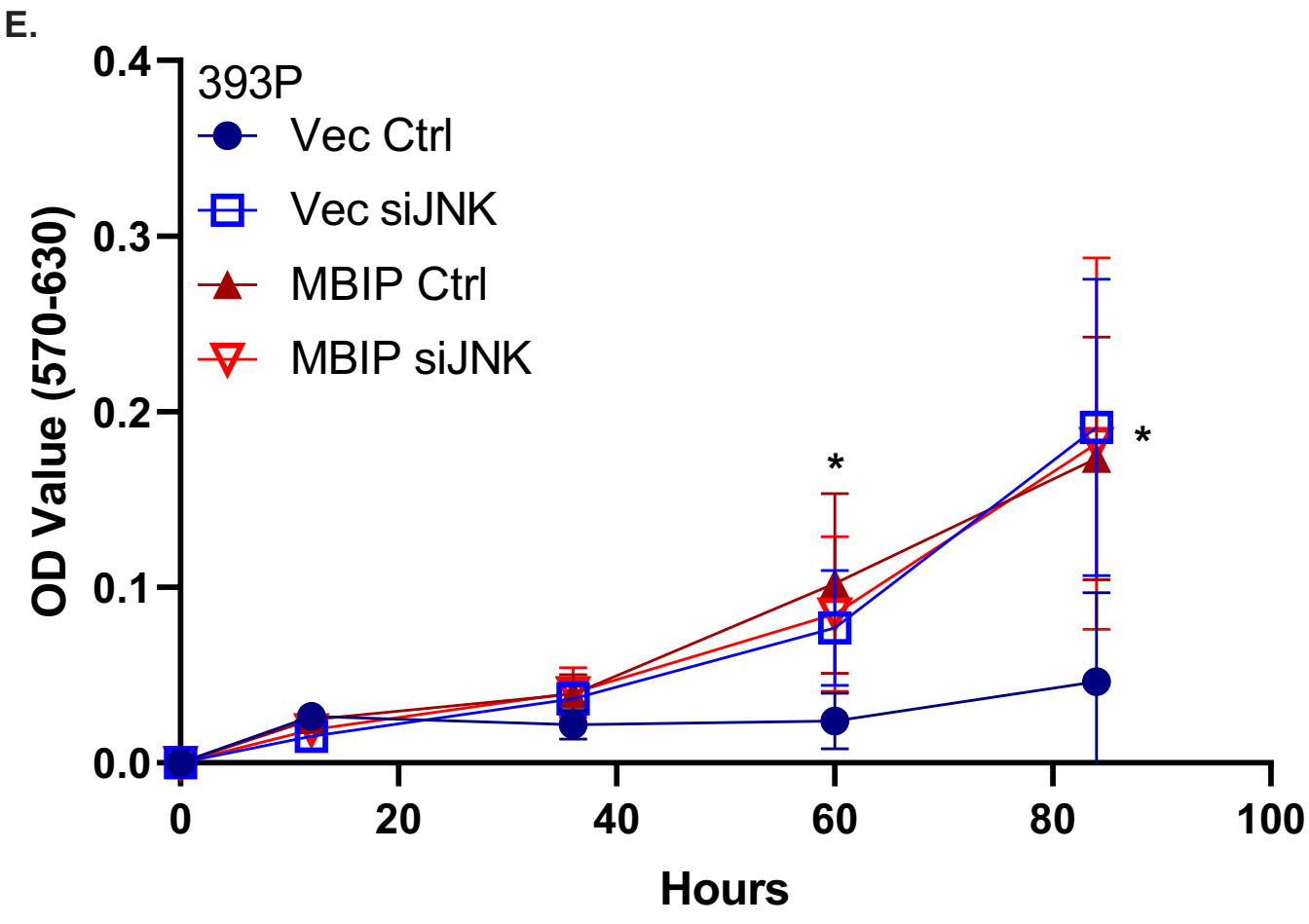
E.
393P
Vec Ctrl
Vec siJNK
MBIP Ctrl
MBIP siJNK
OD Value (570-630)
0.4
0.3
0.2
0.1
0.0
0
20
40
60
80
100
Hours

Figure S4. (A) RT-qPCR analysis of MBIP and JNK substrates upon treatment with JNK inhibitor, SP600125 in 393P MBIP-overexpressing cells. JNK inhibition represses known JNK targets. **(B)** siJNK-mediated knockdown of JNK downregulates MMPs in 393P MBIP-overexpressing cells. **(C)** siJNK-mediated knockdown of JNK downregulates JNK targets, and EMT markers in 393P MBIP-overexpressing cells. **(D)** Repression in MBIP-mediated migration and invasion upon JNK knockdown in 393P MBIP-overexpressing cells. **(E)** MTT assays show no change in proliferation upon JNK repression in 393P-MBIP overexpressing cells as measured by OD value between 570-630 nm. Data is represented as mean ± SEM. *P<0.05, and ***P<0.001.

Figure S5

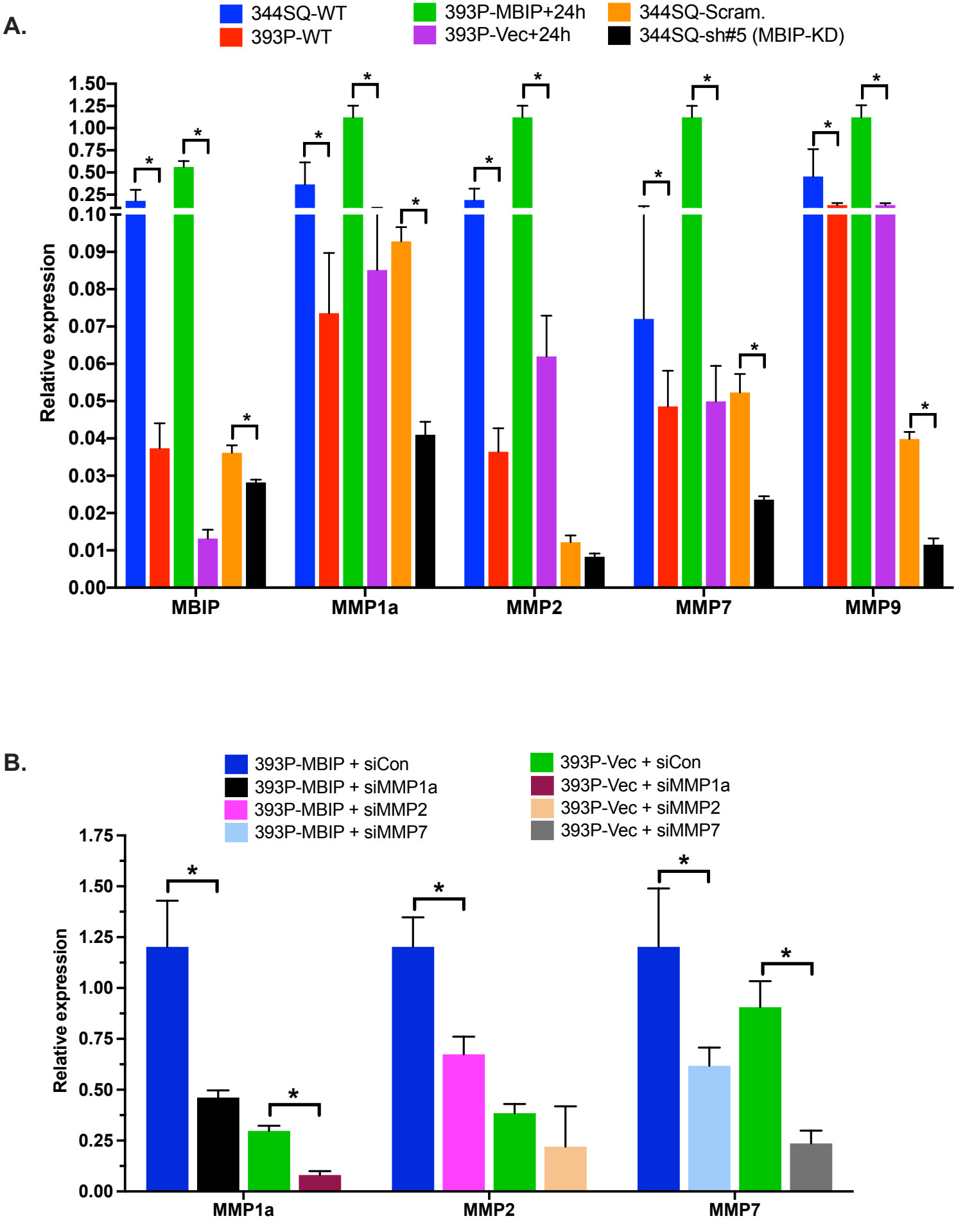
A.
344SQ-WT
393P-WT
393P-MBIP+24h
393P-Vec+24h
344SQ-Scram.
344SQ-sh#5 (MBIP-KD)
Relative expression
MBIP
MMP1a
MMP2
MMP7
MMP9
B.
393P-MBIP + siCon
393P-MBIP + siMMP1a
393P-MBIP + siMMP2
393P-MBIP + siMMP7
393P-Vec + siCon
393P-Vec + siMMP1a
393P-Vec + siMMP2
393P-Vec + siMMP7
Relative expression
MMP1a
MMP2
MMP7

Figure S5

C.

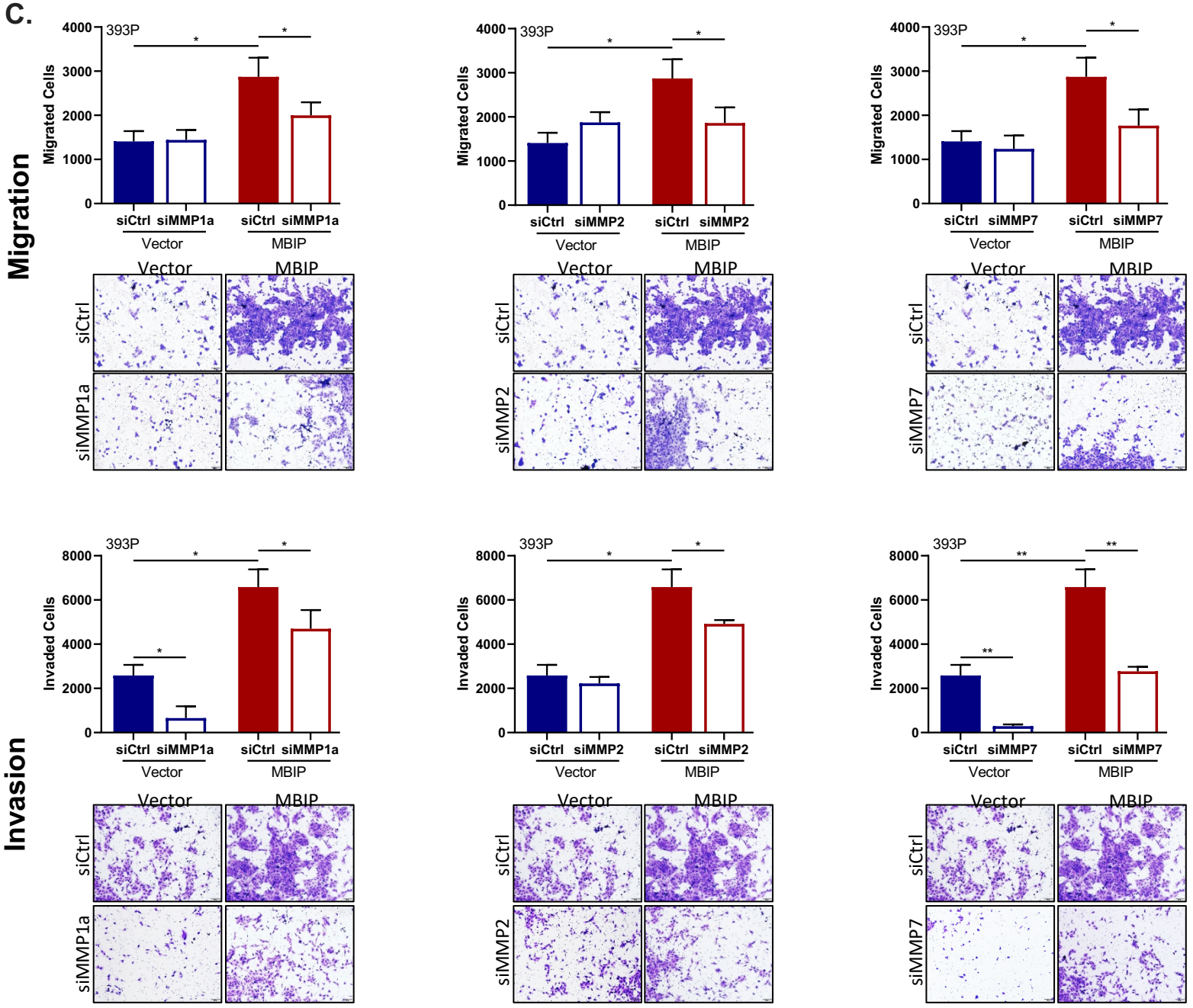
Migration
Invasion
393P
Migrated Cells
Invaded Cells
siCtrl
siMMP1a
siMMP2
siMMP7
Vector
MBIP

Figure S5

D.

3D assay with si-MMP7 transfection

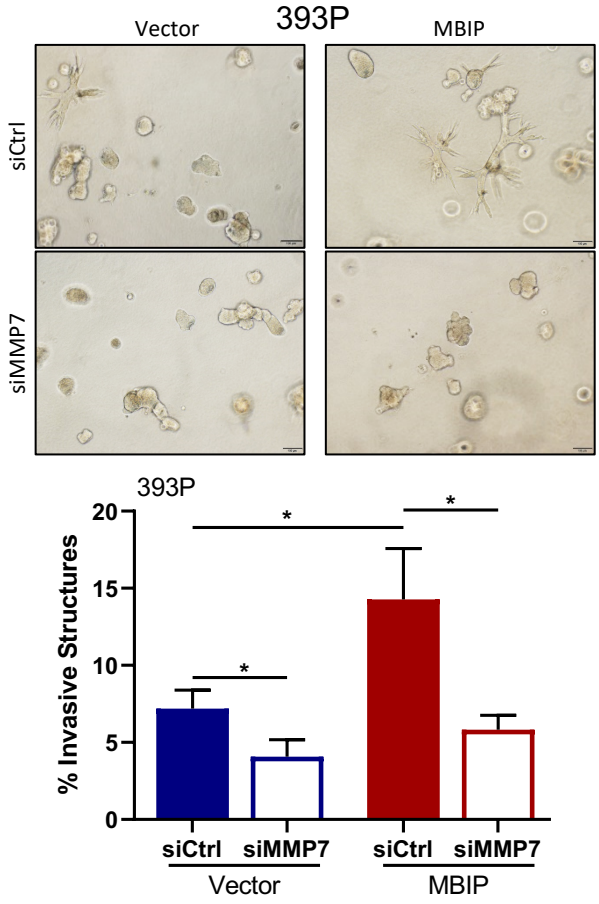

E.

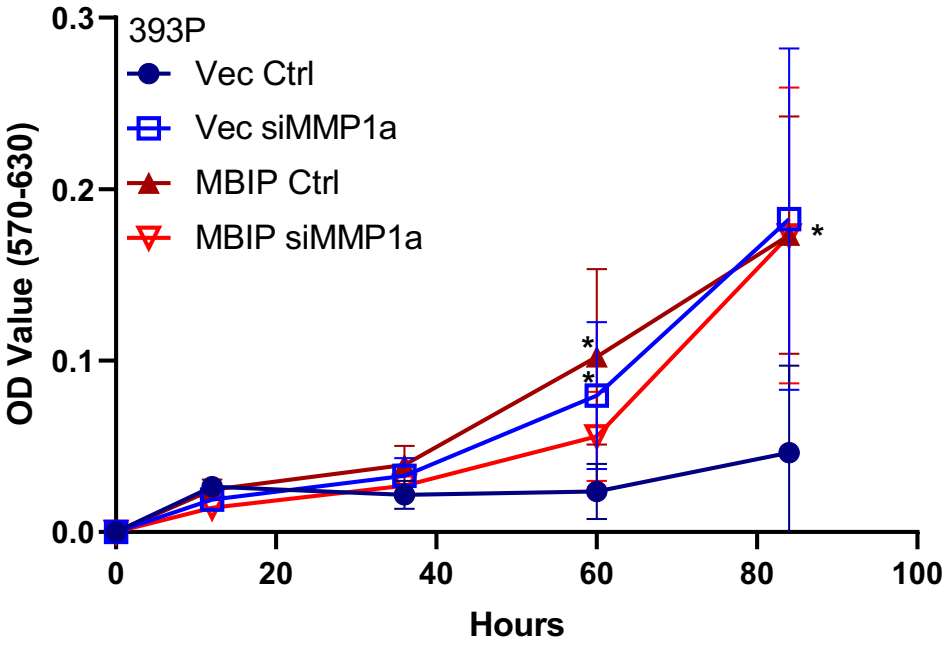

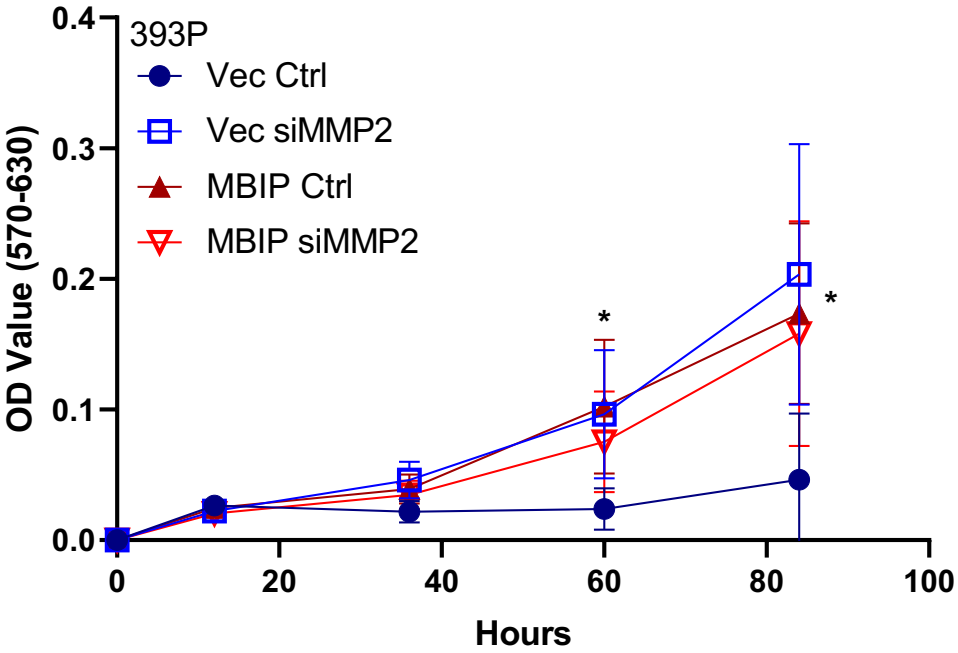

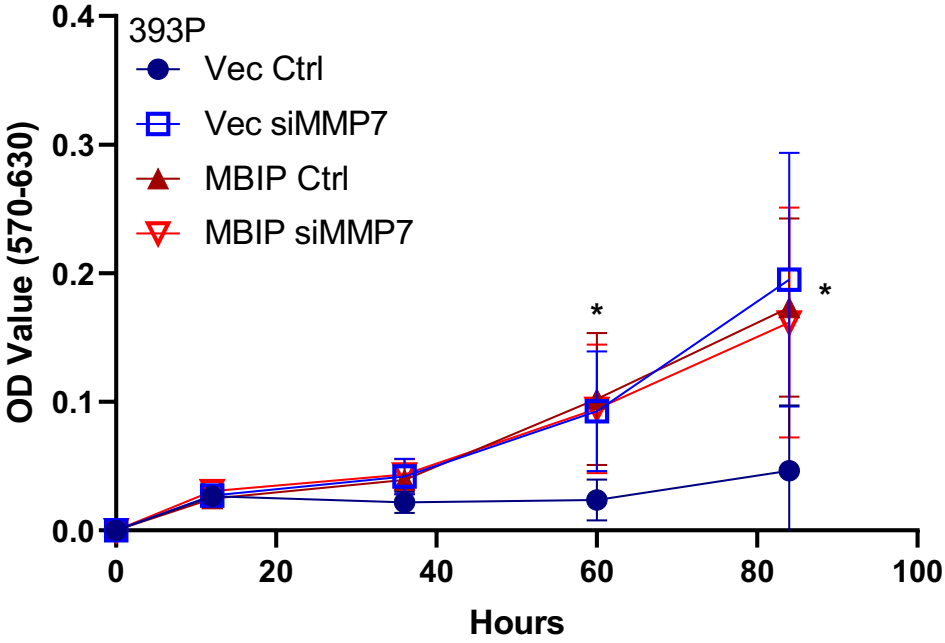

Figure S5. (A) RT-qPCR analysis shows higher MMP expression levels in metastatic/mesenchymal 344SQ and MBIP-overexpressing 393P cells, and lower levels in MBIP knockdown 344SQshMBIP cells compared to their respective controls. **(B)** Knockdown of MMPs in 393P MBIP-overexpressing cells, using MMP-specific siRNAs were validated by RT-qPCR. **(C)** MMP knockdown represses MBIP-mediated 2D migration and invasion of MBIP overexpressing 393P cells. **(D)** MMP knockdown represses MBIP-mediated 3D-invasion phenotype of MBIP overexpressing 393P cells. **(E)** MTT assays show no change in cellular proliferation upon MMP knockdown as measured by OD value between 570-630 nm. Data is represented as mean ± SEM. *P<0.05, and ***P<0.001.

Figure S6

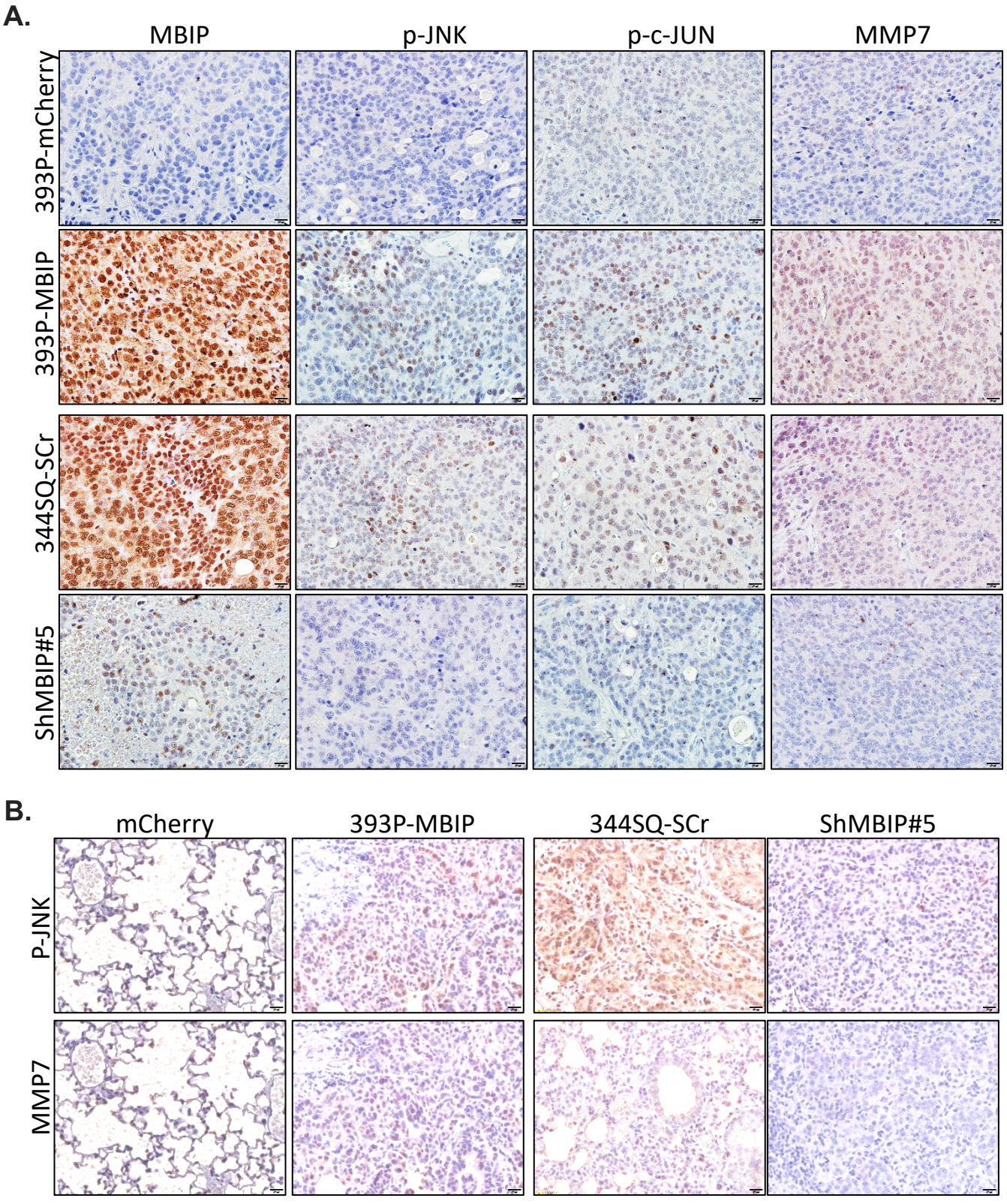
A.
MBIP
p-JNK
p-c-JUN
MMP7
393P-mCherry
393P-MBIP
344SQ-SCr
ShMBIP#5
B.
mCherry
393P-MBIP
344SQ-SCr
ShMBIP#5
P-JNK
MMP7

Figure S6

C.

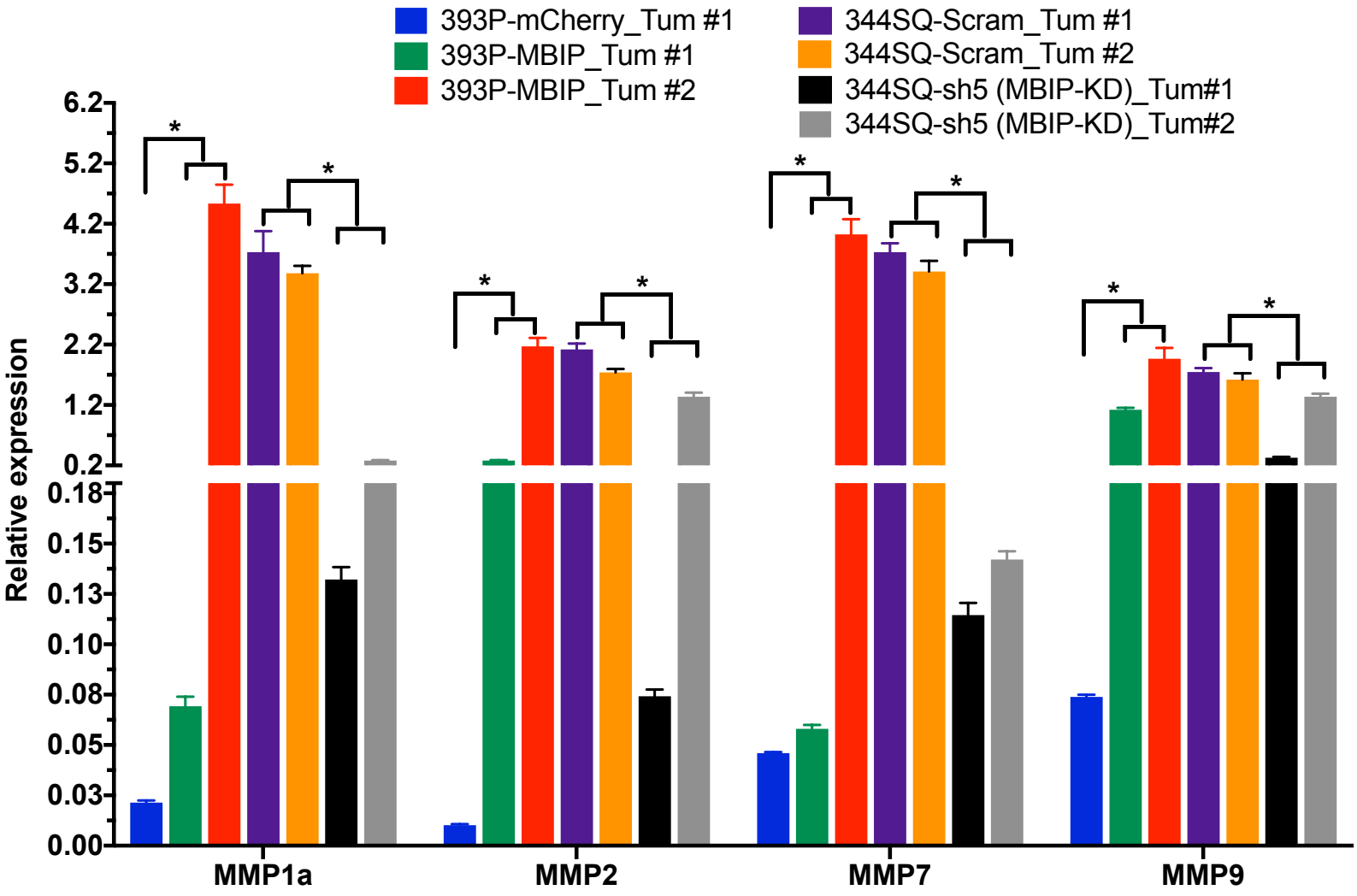

Figure S6. (A-B) Representative IHC staining for p-JNK, p-c-Jun and MMP7 in primary tumors or lung metastatic nodules in **(A)** Primary tumors or **(B)** metastatic lesions from mice injected with control and MBIP overexpressing 393P cells or control and MBIP knockdown 344SQ cells, analyzed with antibodies against the p-JNK, p-c-Jun and MMP7. Scale bar = 100 μm. **(C)** RT-qPCR analysis for MMP levels (MMP1a, MMP2, MMP7 and MMP9) in subcutaneous tumors from control and MBIP overexpressing 393P cells or control and MBIP knockdown 344SQ cells. MMP expression was regulated by MBIP levels. Data is represented as mean ± SEM. *P<0.05, and ***P<0.001.

Supplementary Materials and Methods

Constructs and reagents shRNA details (shMBIP; clone ID TRCN0000124805, TRCN0000124807, Scramble control). ON-TARGETplus siRNA SMARTPools targeting individual genes were purchased from GE-Dharmacon (now Horizon Discovery) and transfected using Lipofectamine RNAiMAX Transfection Reagent (ThermoFisher Scientific) as per manufacturer's protocol.

Wound healing assay. The average distance of the migrating cells was observed using inverted microscopy (Leica Microsystems, Germany) at start time 0 and after 24 h. The migration rate was expressed as the migrated distance of the cells in the experimental group to that of the control group.

Migration and invasion assay. Transwell chambers (8 μm pore polycarbonate, Corning Costar, USA) were used for migration assays and these chambers which were pre-coated with the diluted BD Matrigel™ basement membrane matrix (BD Biosciences, Bedford, MA, USA) were used for invasion assays. Cells were plated at 5×10^4 cells/chamber in serum-free RPMI medium in the upper chamber with complete media in the lower chamber as chemoattractant. 3 chambers were used per cell line/condition. Cells were allowed to migrate/invade for 16 hours, after which the membrane was stained with crystal violet and all residual cells on the upper membrane surface, which did not migrate/invade, were cleaned with a cotton swab. After air drying, the lower surface of the chamber membrane, with the stained (migrated/invaded) cells were viewed under an inverted microscope at 4X magnification. 5 independent fields were photographed per chamber and ImageJ was used to count the cells. Results are presented as average cells per field or per chamber (as mentioned in axis legends).

Animal studies. 8-10 week old 129/Sv mice were used for the *in vivo* experiments.

3D Spheroid assay. As previously published, to quantify the invasion in 3D matrix, we seed 1500 cells per well (3-4 wells/cell line or condition). At day 6 after plating, the spheroids are counted while viewing at 4X magnification on an inverted microscope. 100 – 200 total spheroids are counted per well. Spheroids with invasive projections as shown in the representative images are then represented as percentage of total counted spheroids. The data shown are average percentages from 4 wells/condition .

Western blotting. Whole cell lysates and tissue lysates were prepared using radioimmunoprecipitation assay (RIPA) buffer (Cell Signaling, USA). Protein concentrations were determined using Pierce™ BCA protein assay kit (Thermo scientific, USA). Protein samples were subjected to SDS-PAGE, transferred to a nitrocellulose membrane, which was then blocked with 5% skim milk in TBST (10 mM Tris, 100 mM NaCl, and 0.1% Tween 20) for 1 h at room temperature. Membranes were then probed with specific primary antibodies for (MBIP, p-JNK, JNK, p-c-Jun, c-Jun, MMP7) and peroxidase-conjugated secondary antibodies purchased from cell signaling and Millipore (USA). Blots were visualized using an ECL detection system.

Immunohistochemistry Primary antibodies used were: rabbit anti-mouse polyclonal antibody MBIP (SAB1407501, Millipore, dilution 1:1000), mouse anti-rabbit monoclonal antibody E-cadherin (3195s, cell signaling, dilution 1:1000) and N-cadherin (13116s, cell signaling, dilution 1:1000, MMP7 (71031s, cell signaling, dilution 1:1000) overnight at 4°C. Secondary antibodies used were: anti-rabbit (Dako Swine #E0353, 1:300).

ANTIBODIES

	Dilution.	Company
Western blot		
MBIP	1:500	Thermofisher Scientific
p-JNK	1:1000	Cell signaling
JNK	1:1000	Cell signaling
p-c-JUN	1:1000	Cell signaling
MMP7	1:1000	Cell signaling
IHC/IF antibodies		
E-Cad	1: 500	Cell signaling
N-Cad	1:500	Cell signaling
Vim	1:500	Abcam
Zeb1	1:500	Novus biologicals
Secondary antibody		
goat anti-mouse	1:300	Dako
Alexa fluor 488	1:200	Thermofisher
Vectashield DAPI	Drop	Sigmaaldrich

qRT-PCR Primers	
MBIP	F: CATACGGACCACAGACTAGACC
	R: ATGTCTCTTGGCACTGGACCAC
Mbip	F: GGTCACAAACCTACAGGCATGC
	R: GGTAGATGTCTCTTGGTACTGGG
c-JUN	F: CCTTGAAAGCTCAGAACTCGGAG
	R: TGCTGCGTTAGCATGAGTTGGC
Smad4	F: CAGCCATAGTGAAGGACTGTTGC
	R: CCTACTTCCAGTCCAGGTGGTA
Sp1	F: ACGCTTCACACGTTCGGATGAG
	R: TGACAGGTGGTCACTCCTCATG
Elk1	F: GGAACAAGCTCTGGTCTTCAGG
	R: GGACTCAGAGTGCTCCAGAAATG
Alf2	F: CCATGCTAGGTGACGGCTCTTC
	R: GCGAGCCATTAACCTCAGATCC
Pax6	F: CTGAGGAACCAGAGAAGACAGG
	R: CATGGAACCTGATGTGAAGGAGG
MMP1	F: ATGAAGCAGCCCAGATGTGGAG
	R: TGGTCCACATCTGCTCTTGGCA
MMP2	F: CAAGGATGGACTCCTGGCACAT
	R: TACTCGCCATCAGCGTTCCCAT
MMP3	F: CTCTGGAACCTGAGACATCACC
	R: AGGAGTCCTGAGAGATTTGCGC
MMP7	F: AGGTGTGGAGTGCCAGATGTTG
	R: CCACTACGATCCGAGGTAAGTC
MMP9	F: GCTGACTACGATAAGGACGGCA
	R: TAGTGGTGCAGGCAGAGTAGGA
MMP13	F: GATGACCTGTCTGAGGAAGACC
	R: GCATTTCTCGGAGCCTGTCAAC